1 **High organic carbon burial but high potential for methane ebullition in the**

2 **sediments of an Amazonian hydroelectric reservoir**

3 Gabrielle R. Quadra[1]✉, Sebastian Sobek[2], José R. Paranaíba[1], Anastasija Isidorova[2],

4 Fábio Roland[1], Roseilson do Vale[3], Raquel Mendonça[1]

5 [1] Laboratório de Ecologia Aquática, Programa de Pós-Graduação em Ecologia,

6 Universidade Federal de Juiz de Fora, 36036 900, Brazil.

7 [2] Department of Ecology and Genetics, Limnology, Uppsala University, 752 36,

8 Sweden.

9 [3] Universidade Federal do Oeste do Pará, Instituto de Engenharia e Geociências, 68040

10 255, Brazil.

11 ✉gabrielle.quadra@ecologia.ufjf.br

12 **Abstract**

13 Reservoir sediments sequester significant amounts of organic carbon (OC), but at the

14 same time, high amounts of methane (CH_4) can be produced and emitted during the

15 degradation of sediment OC. While the greenhouse gases emission of reservoirs has

16 received a lot of attention, there is a lack of studies focusing on OC burial. In particular,

17 there are no studies on reservoir OC burial in the Amazon, even though hydropower is

18 expanding in the basin. Here we present results from the first investigation of OC burial

19 and CH_4 concentrations in the sediments of an Amazonian hydroelectric reservoir. We

20 performed sub-bottom profiling, sediment coring and sediment pore water analysis in

21 the Curuá-Una reservoir (CUN; Amazon, Brazil) during rising and falling water

22 periods. Spatially resolved average sediment accumulation rate was 0.6 cm yr^{-1} and a

23 average OC burial rate was 91 g C m^{-2} yr^{-1}. This is the highest OC burial rate on record

24 for low-latitude hydroelectric reservoirs. Such high rate probably results from a high

25 OC deposition onto the sediment, which compensates the high OC mineralization at 28-

26 30°C water temperature. Elevated OC burial was found near the dam, and close to

27 major river inflow areas. C:N ratios between 10.3 and 17 (average ± SD: 12.9 ± 2.1)

28 suggest that both land-derived and aquatic OC accumulate in CUN sediments. About

29 23% of the sediment pore water samples had dissolved CH_4 above the saturation

30 concentration. This represents a higher share than in other hydroelectric reservoirs,

31 indicating a high potential for CH_4 ebullition, particularly in river inflow areas.

32 **Keywords:** Amazon, carbon cycling, C:N ratio, dam, pore water, river inflow

33 **Introduction**

34   Although freshwater ecosystems represent a small fraction of the global area

35 (~4% of terrestrial area) (Downing et al., 2012; Verpoorter et al., 2014), they play an

36 important role in the global carbon cycle, both emitting carbon to the atmosphere and

37 burying carbon in the sediments (Cole et al., 2007; Tranvik et al., 2009). Many studies

38 have been conducted on inland water carbon emissions, while the organic carbon (OC)

39 burial in inland water sediments is comparatively understudied on a global scale

40 (Raymond et al., 2013; Mendonça et al., 2017). Since a part of the buried OC may offset

41 a share of greenhouse gas emission, it is essential to include OC burial in the carbon

42 balance of inland water ecosystems (Kortelainen et al., 2013; Mendonça et al., 2017).

43   Freshwater OC burial rate varies both in space and time due to many factors,

44 such as land cover, hydrological conditions, OC and nutrient input and climate change

45 (Radbourne et al., 2017; Stratton et al., 2019). Several studies have shown that

46 reservoirs bury more OC per unit area than lakes, rivers and oceans (Mulholland and

47 Elwood, 1982; Mendonça et al., 2017), which may be attributed to the high

48 sedimentation rate caused by the extensive sediment trapping when water flow is

49 dammed (Vörösmarty et al., 2003). Considering the importance of reservoirs as a

50 carbon sink (~28 to 55% of total inland water OC burial; Mendonça et al., 2017) and the

51 increasing number of hydroelectric dams (Zarfl et al., 2015), the limited number of

52 studies on OC burial in reservoirs severely hampers the understanding of this important

53 component in the carbon balance of the continents (Mendonça et al., 2017). In

54 particular, large regions of the Earth are at present completely unsampled concerning

55 inland water carbon burial. Approximately 90% of the sites sampled for carbon burial

56 are in North America and Europe, while there are only few measurements in South

57 American, African and Asian countries (Mendonça et al., 2017).

58   To the best of our knowledge, OC burial has so far not been studied in an

59 Amazonian reservoir. However, it is likely that reservoirs in tropical rain forest areas

60 bury OC at a comparatively high rate, as temperature and runoff were identified as

61 important drivers of OC burial in lakes and reservoirs (Mendonça et al., 2017). Indeed,

62 OC burial in Amazonian floodplain lakes was reported to be much higher than in other

63 lakes (Sanders et al., 2017). Moreover, many new hydropower dams are planned in the

64 Amazon due to the high potential of the area for hydroelectricity (da Silva Soito and

65 Freitas, 2011; Winemiller et al., 2016). However, there is currently no data to gauge the

66 potential effect of hydropower expansion in the Amazon on carbon burial.

67   Besides the significant potential of trapping OC in the sediment, reservoirs can

68 be strong sources of methane (CH_4) to the atmosphere (Deemer et al., 2016). Several

69 studies have shown a positive relationship between CH_4 production and temperature in

70 freshwater ecosystems (Marotta et al., 2014; Wik et al., 2014; Yvon-Durocher et al.,

71 2014; DelSontro et al., 2016; Aben et al., 2017), and also organic matter supply to

72 sediment is an important regulator of CH_4 production and emission (Segers, 1998;

73 Sobek et al., 2012; Grasset et al., 2018). Thus, tropical reservoirs, especially those

74 situated in highly productive humid tropical biomes, such as the Amazon, may produce

75 more CH_4 than temperate ones due to higher annual temperatures and availability of

76 organic matter in their sediments (Barros et al., 2011; Mendonça et al., 2012; Fearnside

77 and Pueyo, 2012; Almeida et al., 2013), although highly-emitting reservoirs can also be

78 situated in temperate regions (Deemer et al., 2016). Further, in many reservoirs, CH_4

79 ebullition (i.e., emission of gas bubbles) is an important or dominant emission pathway,

80 but it is very difficult to measure due to its strong variability in space and time

81 (McGinnis et al., 2006; Deemer et al., 2016). Measurements of dissolved CH_4

82 concentration in sediment pore water may, therefore, help to identify if ebullition is

83   likely to occur (CH_4 concentrations close to the sediment pore water saturation), and

84   thus to judge if the sediments act mainly as carbon sinks, or also as CH_4 sources. While

85   CH_4 emission typically constitutes a very small flux in terms of carbon mass, it is highly

86   relevant to climate since CH_4 is a ~34 times stronger greenhouse gas than CO_2 (IPCC,

87   2013). The transformation of sediment OC (i.e. previously fixed CO_2) to atmospheric

88   CH_4 therefore represents an amplification of radiative forcing in the atmosphere.

89   Both OC burial and CH_4 production take place in sediments. Here, we present

90   results of a study approaching these processes on sediments of an Amazonian

91   hydroelectric reservoir during hydrologically different seasons, which was motivated by

92   an absence of such studies even though sediment carbon processing in Amazonian

93   reservoirs may potentially be high. We aimed at providing a spatially-resolved

94   quantification of OC burial, as well as a mapping of CH_4 saturation in the sediment

95   porewater, which is indicative of the potential occurrence of CH_4 ebullition. Thereby,

96   this study is intended to contribute to improved understanding of the potential

97   biogeochemical effects of the current expansion of hydropower (Almeida et al., 2019)

98   on the Amazonian carbon budget.

99   **Material and methods**

100   *Study area*

101   Curuá-Una is an Amazonian reservoir (CUN; 2°50′ S 54°18′ W) located in the

102   Pará state (North of Brazil), created in 1977, and used mainly to produce energy. The

103   average water depth of CUN is 6 m (Fearnside, 2005; Paranaíba et al., 2018) and it has

104   a maximum flooded area of 72 km^2 (Duchemin et al., 2000; Fearnside, 2005). The main

105   tributary is the Curuá-Una River, contributing with most of the reservoir's water

106   discharge (57.4%), but rivers Moju (11.7%), Mojuí (4.4%), Poraquê (3.2%) and other

107   small ones (2.9%) are also important (Fearnside, 2005). While tropical rain forest

108   covers 90.8% of the total CUN catchment area, managed lands, which covers 8.9% of

109   the total catchment, contribute with a high share (up to 41%) of the land cover in some

110   sub-catchments (**Fig. 1**).

111   The reservoir is characterized by a high amount of flooded dead trees (area with

112   trees covers ~90% of the total reservoir area), which may be expected to decrease water

113   flow and promote sedimentation. According to a previous study (Paranaíba et al., 2018),

114   CUN is oligotrophic (total nitrogen (TN): 0.7 mg L^{-1}, average; total phosphorus (TP):

115   0.02 mg L^{-1}, average), the surface water is warm (average $\pm$ SD: 30.1 $\pm$ 1.4 °C), slightly

116   acidic (pH of 6.1 $\pm$ 0.7), with low conductivity (16 $\pm$ 11 μS cm^{-1}) and moderately

117   oxygenated (6.7 $\pm$ 1.9 mg L^{-1}).

118   *Sampling*

119   We carried out two samplings in the CUN reservoir. In February 2016, during

120   the rising water period (**Fig. S1**), we used an Innomar SES-2000 parametric sub-bottom

121   profiler operating at 100 kHz (primary frequency) and 15 kHz (secondary frequency) to

122   determine the bathymetry and sediment thickness from which we planned to acquire

123   spatially resolved sediment accumulation rates and OC burial rate, similar to Mendonça

124   et al. (2014). Sediment thickness was difficult to observe with the sub-bottom profiler,

125   though, presumably because of the widespread presence of gas bubbles in the sediment

126   which reflect the sound waves very efficiently, preventing them from reaching the sub-

127   bottom layer. Therefore, OC burial rates were determined from sediment cores only. In

128   September 2017, during the falling water period (**Fig. S1**), additional sediment cores

129   were then taken to cover the reservoir as much as possible.

130   We took a total of 114 sediment cores during the two sampling occasions,

131   approximately evenly distributed along the reservoir, both longitudinally and laterally,

132   to measure sediment thickness and, thus, estimate sediment accumulation and OC burial

133   rates (**Fig. 1**, **Table S1**). Cores were retrieved using a gravity corer equipped with a

134   hammer device (UWITEC, Mondsee, Austria) to sample the entire sediment layer,

135   including the pre-flooding material. The layer of transition between post- and pre-

136   flooding material was visually identified. Visual identification is possible because the

137   moment when the reservoir was flooded is the onset of a lacustrine depositional regime,

138   which is characterized by different sediment texture and composition in relation to the

139   pre-flooding soil or fluvial sediment (**Fig. S2**). The thickness of the post-flooding

140   sediment was noted in all cores and used to calculate sediment accumulation rates ('data

141   analysis'). Nineteen sediment cores, from sites spread out evenly over the reservoir

142   were sliced in 2 cm thick slices and dried at 40 ℃ for further laboratory analysis. The

143   samples were weighed before and after drying and the results are, then, expressed in dry

144   weight.
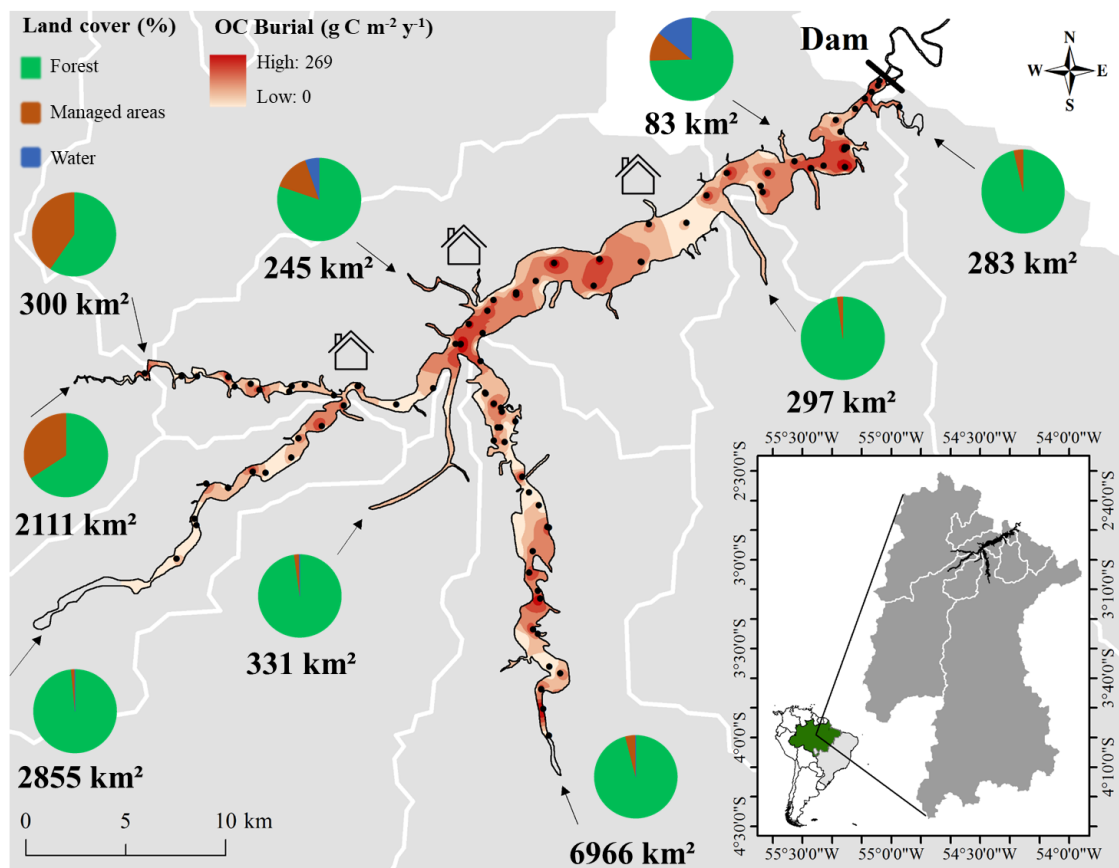
Figure 1. Organic carbon burial rate (OC burial; g C m^{-2} yr^{-1}) of the Curuá-Una

reservoir. The circles show the land cover of each sub-catchment, delineated by white

lines. The numbers near the circles show the area in km² for each sub-catchment. The

black dots represent the sediment sampling sites to estimate OC burial rates. The arrows

represent the main river inflows. The houses represent settlements at the reservoir. The

bottom-right map shows the location of the reservoir in Brazil (the green area is the

Brazilian Amazon region) and the total extension of each sub-catchment.

    In both sampling campaigns, targeted to rising and falling water periods,

sediment cores were taken for the analysis of pore water CH_4 concentration profiles (n =

16 in February 2016 and n = 9 in September 2017). Of the nine cores taken in

September 2017, eight were situated at sites previously sampled in February 2016, to

compare the CH_4 concentrations between sampling occasions. It is difficult to sample

158   the exact same location at different periods due to the water level changes, GPS error

159   and boat drifting. Thus, the repeated samplings at these eight sites were within < 100 m

160   distance.

161   Water temperature and dissolved oxygen profiles were measured with a

162   multiparameter sonde (YSI 6600 V2) in a total of 28 depth profiles, distributed across

163   the reservoir at both sampling occasions. Air pressure and temperature were measured

164   with a portable anemometer (Skymaster SpeedTech SM-28, accuracy: 3%), water depth

165   was measured with a depth gauge (Hondex PS-7), and sediment temperature with a

166   thermometer (Incoterm), which was inserted into the sediment right after core retrieval.

167   *Carbon and nitrogen analysis*

168   OC and TN concentrations were determined in a sub-set of 19 cores, distributed

169   evenly across the reservoir area. In each of these cores, the first and second layers (0 to

170   4 cm deep, containing the fresher OC), the last sediment layer above the pre-flooding

171   soil surface (containing the older OC) and one sample every ~8 cm in between (OC of

172   intermediate age) were analyzed. This selection of layers for carbon and nitrogen

173   analyses was motivated by the exponential decrease of OC mass loss rates during

174   sediment degradation (Middelburg et al., 1993; Gälman et al., 2008). Linear

175   interpolation was used to derive OC and TN concentrations of layers that were not

176   measured.

177   Dried sediment samples were ground in a Planetary Ball Mill (Retsch PM 100)

178   equipped with stainless steel cup and balls. Sediment was packed in pressed tin capsules

179   and analyzed for TC and TN with a Costech 4010 elemental analyzer. The molar carbon

180   to nitrogen (C:N) ratio in the surface layers was then calculated. The presence of

181   carbonates was checked in the samples qualitatively by adding drops of acid and

182   checking visually for reaction. No evidence of solid carbonates was found, thus

183   measurements of TC correspond to OC.

184   *CH_4 concentration in pore water*

185   The CH_4 concentration in pore water was measured according to Sobek et al.,

186   (2012) to determine if CH_4 is close to saturation concentration and, thus, prone to form

187   gas bubbles. The saturation concentration, calculated here from temperature and

188   pressure along the sediment profiles, represents the maximum concentration that

189   dissolves in pore water, above which bubbles are formed. The presence of gas bubbles

190   is indicative for an elevated probability of CH_4 ebullition, but not necessarily relates

191   quantitatively to ebullition flux, since ebullition flux to the atmosphere is also

192   dependent on water depth, sediment grain size, and pressure fluctuations (McGinnis et

193   al., 2006; Maeck et al., 2014; Liu et al., 2016). The top 20 cm (February 2016) or 40 cm

194   (September 2017) of the sediment cores were sampled every 2 cm. Deeper sediment

195   was sampled every 4 cm until the bottom or pre-flooding material. Using a core liner

196   with side ports, 2 ml of sediment were collected using a syringe with a cut-off tip, added

197   to a 25 mL glass vial with 10 ml of distilled water, and closed with a 10 mm thick butyl

198   rubber stopper. The slurry (2 mL sediment + 10 mL distilled water) was equilibrated

199   with 13 mL headspace of ambient air (void volume of the glass vial) immediately after

200   sampling by vigorously shaking the glass vial, and then the headspace was transferred

201   to another syringe. The headspace was stored in the syringe, closed with a gas-tight

202   valve, and then analyzed for CH_4 concentration within the same day using an

203   Ultraportable Greenhouse Gas Analyzer (UGGA, Los Gatos Research) with a custom-

204   made sample injection port. Then, the resulting peaks were integrated using R software

205   (RStudio Version 1.1.383). The CH_4 concentration in the pore water was calculated

206   from the headspace CH_4 concentration, based on the Henry's law constants. The

207   saturation concentration of CH_4 in each sediment layer was calculated based on air

208   pressure, water depth, sediment temperature, and sample depth within the sediment

209   core. The sediment layers with CH_4 concentrations above 100% saturation were

210   considered as prone to ebullition. This is a conservative assumption because it is likely

211   that a part of the CH_4 in the sediment was lost to the atmosphere due to pressure drop

212   during core retrieval, as well as during sample processing.

213   *Data analysis*

214   The average sediment accumulation rate (SAR; cm yr^{-1}) was calculated for each

215   of the 114 cores by dividing the thickness of the post-flooding sediment (cm) by the

216   years since the reservoir construction (39 years in 2016 or 40 years in 2017), according

217   to the equation:

218
$$Sediment\ accumulation\ rate = \frac{\text{sediment thickness}}{\text{reservoir age}}$$

219   This approach returns the average sediment accumulation rate over the lifetime

220   of the reservoir (Renwick et al., 2005; Kunz et al., 2011; Mendonça et al., 2014; Quadra

221   et al., 2019), and therefore incorporates any short-term variability in sediment

222   deposition, for example, caused by an episodic change in sediment load or internal

223   sediment movement. The large amount of core samples distributed evenly across the

224   reservoir body also covers the spatial variability in sediment deposition, for example

225   due to sediment focusing (sediment movement with preferential deposition in deeper

226   areas).

227   OC burial rates (g C m^{-2} yr^{-1}) were calculated for the sub-set of 19 sites where

228   OC content was analyzed. OC mass (g C) in each sediment slice was calculated as OC

229   content (g C g^{-1}) multiplied by dry sediment mass (g). Total OC mass (g C) in the cores

230   was the sum of OC mass in all post-flooding sediment layers. Then, the average OC

231   burial rate (g C m^{-2} yr^{-1}) for each of these 19 sites was calculated dividing the total OC

232   mass in post-flooding sediment (g C) by the core surface area (2.8 x 10^{-3} m^2) and the

233   reservoir age (yr) at the sampling dates, according to the equation:

234
$$Organic\ carbon\ burial\ rate\ = \frac{OC\ in\ reservoir\ sediment}{core\ area\ \times reservoir\ age}$$

235   The empirical relationship between SAR and OC burial rate (see Results; y =

236   159 x - 4.4; R^2 = 0.87; Fig. S3) was used to estimate the OC burial rate (g C m^{-2} yr^{-1}) for

237   the remaining 95 coring sites where OC content was not analyzed.

238   To produce spatially-resolved maps of SAR and OC burial rate, the data from

239   the 114 cores were interpolated to the reservoir area using the Inverse Distance

240   Weighted algorithm (IDW, cell size of approximately 22 m x 22 m). From the spatially-

241   resolved average OC burial rate, the reservoir age (40 years) and total flooded area (72

242   km^2), we calculated the total OC stock in the reservoir sediment. Using the same

243   approach, we interpolated the pore water CH_4 concentration, and C:N ratio for the whole

244   reservoir area. Spatial analyses were performed in ArcGIS 10.3.1 (ESRI).

245   To investigate any potential relationships between the land cover of sub-

246   catchments and the spatial distribution of sediment characteristics and rates, land cover

247   data were derived from maps of 1 km resolution (Global Land Cover Project,

248   GLC2000), made available by the European Commission's science and knowledge

249   service, including 23 land cover classes. The classes found in the CUN watershed were

250   then grouped in three main classes: (1) forest (tree cover, natural vegetation, shrub, and

251   herbaceous cover); (2) managed areas (cultivated and managed areas, cropland and bare

252   areas); (3) and water bodies. The extent of the CUN watershed and sub-catchments were

253   identified using the WWF HydroBASINS tool (HydroSHEDS, 2019).

254   To verify the differences between CH_4 concentrations in the two seasons (rising

255   and falling water), the non-parametric Wilcoxon Test was performed using the software

256   JMP 14.1.0 (SAS).

257   **Results**

258   *Water column profiles*

259   The water column temperature profiles showed a average of 30 ± 1 ºC, 29 ± 1 ºC

260   and 29 ± 2 ºC (average $\pm$ SD) in the surface, the middle and bottom layers, respectively.

261   The dissolved oxygen average was 7 ± 1 mg L^{-1}, 6 ± 1 mg L^{-1} and 5 ± 1 mg L^{-1} in the

262   surface, the middle and bottom layer, respectively. These water profiles suggest that the

263   relatively shallow water column does not develop stable stratification over any extended

264   periods of time, even if short-lived stratification events can occur (**Table S2**).

265   *Sediment accumulation and organic carbon burial rates*

266   SAR in the coring sites (n = 114) varied from 0 to 1.7 cm yr^{-1} (0.6 ± 0.4 cm yr^{-1},

267   95% confidence interval: 0.5-0.7 cm yr^{-1}; **Table S1**). In some areas of rocky or sandy

268   bottom, especially near river inflows and along the main river bed, sediment could not

269   be retrieved with our corer and SAR was considered as zero (total of 10 sites). OC

270   burial rate in the coring sites (n = 114) varied from 0 to 269 g C m^{-2} yr^{-1} (91 ± 61 g C m^{-}

271   ^{1} yr^{-1}, 95% confidence interval: 80-102 g C m^{-1} yr^{-1}; **Table S1**). The highest values of

272   OC burial were observed near the dam, at the confluence of the major inflowing rivers,

273   and in the inflow area of the main tributary, Curuá-Una River (**Fig. 1**). Our sampling

274   was representative of the whole system, from the margins, where there is a greater

275   presence of dead tree trunks, to the river bed, where the sedimentation was lower (**Fig.**

276   **1**). Therefore, the simple average OC burial from the cores resulted in the same average

277   OC burial rate derived from the spatial interpolation (91 g C m^{-1} yr^{-1}). The total burial

278   rate for the CUN reservoir area was 6.5 x 10^{10} g C yr^{-1}, corresponding to an

279   accumulation of 0.3 Tg C in CUN sediments since its construction.

280   *C:N ratio and land cover*

281   The C:N ratio of the surface layers of sediment (n = 19), used as an indicator of

282   organic matter source, varied from 10.3 to 17 (12.9 ± 2.1, **Table S3**, **Fig. 2**). Higher C:N

283   ratios were observed in the dam area and at the river inflows (**Fig. 2**).

284   Tropical rain forest was the dominant land cover in CUN, covering from 60.6 to

285   98.6% of the sub-catchment areas. Managed areas covered 1.4 to 40.9% of the sub-

286   catchments areas, with the higher values occurring in the northwestern tributaries,

287   which were also smaller compared to the southern ones (**Fig. 1**). Water surfaces covered

288   0.3% of the total CUN catchment area (**Table S4**).

289
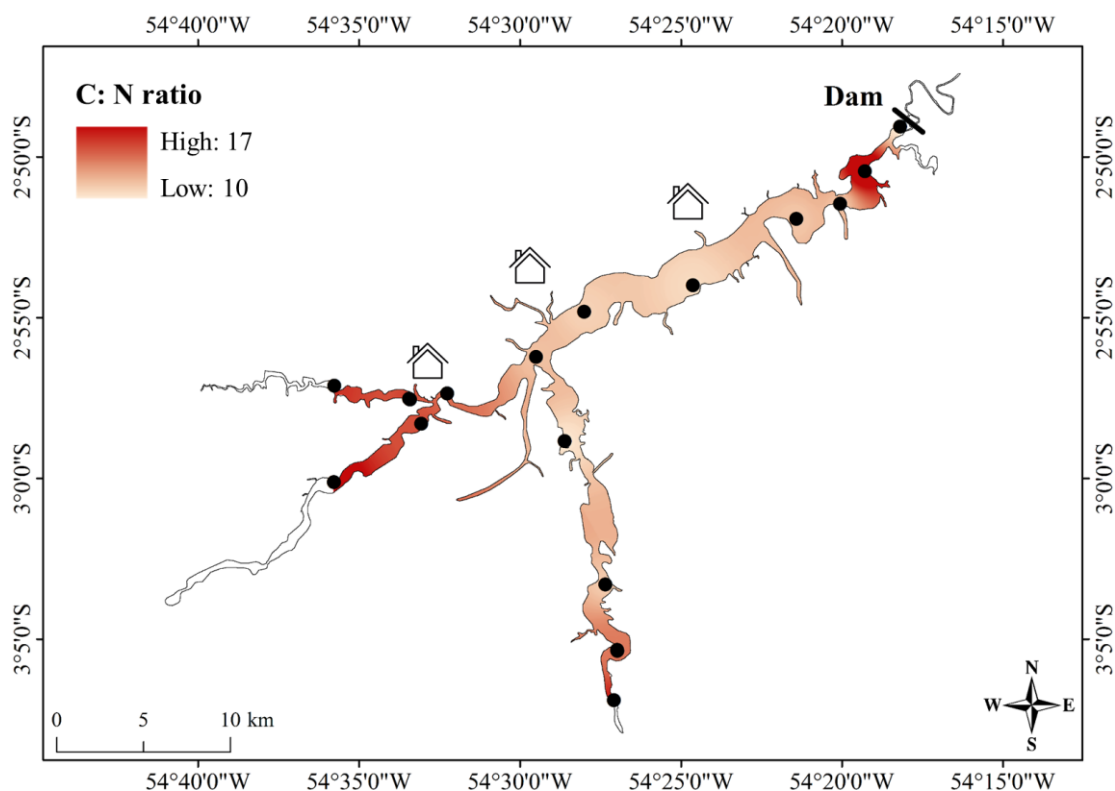
Figure 2. C:N ratio of surface sediment in Curuá-Una reservoir. The black dots

represent the sampling sites. The houses represent the settlements at the reservoir.

Pore water CH₄ profiles and saturation

The overall average CH_4 concentration in pore water from CUN was 1 729 ± 1

939 µmol L^{-1} of CH_4 with similar averages during rising (1 700 ± 1 637 µmol L^{-1} of

CH_4, **Fig. S4**) and falling water (1 764 ± 2 243 µmol L^{-1} of CH_4, **Fig. S4**) periods. At

eight sites, we could make paired observations of CH_4 concentration in sediment pore

water at both rising and falling periods (**Fig. 3**). These data show that the seasonal

difference of CH_4 concentration in pore water was low and not significant (S = 33213, Z

= -1.27863, Prob>|Z| = 0.20). Of the 25 pore water CH_4 profiles, 20 contained at least

one sample with pore water CH_4 above the 100% saturation concentration; of the total

of 386 pore water samples, 90 samples (23%) were above the CH_4 saturation

concentration. Pore water CH_4 saturation was higher in river inflow areas, especially in

304   sampling sites in the Curuá-Una main river. The confluence of the rivers and the dam

305   area were also characterized by high pore water CH_4 (**Fig. 4**). The widespread

306   appearance of gas bubbles in the sediment is in accordance with the sub-bottom profiler

307   data, which for a large part of the reservoir could not be used to identify sub-bottom

308   structures, because of a very strong acoustic reflector in surficial sediment, presumably

309   gas bubbles.
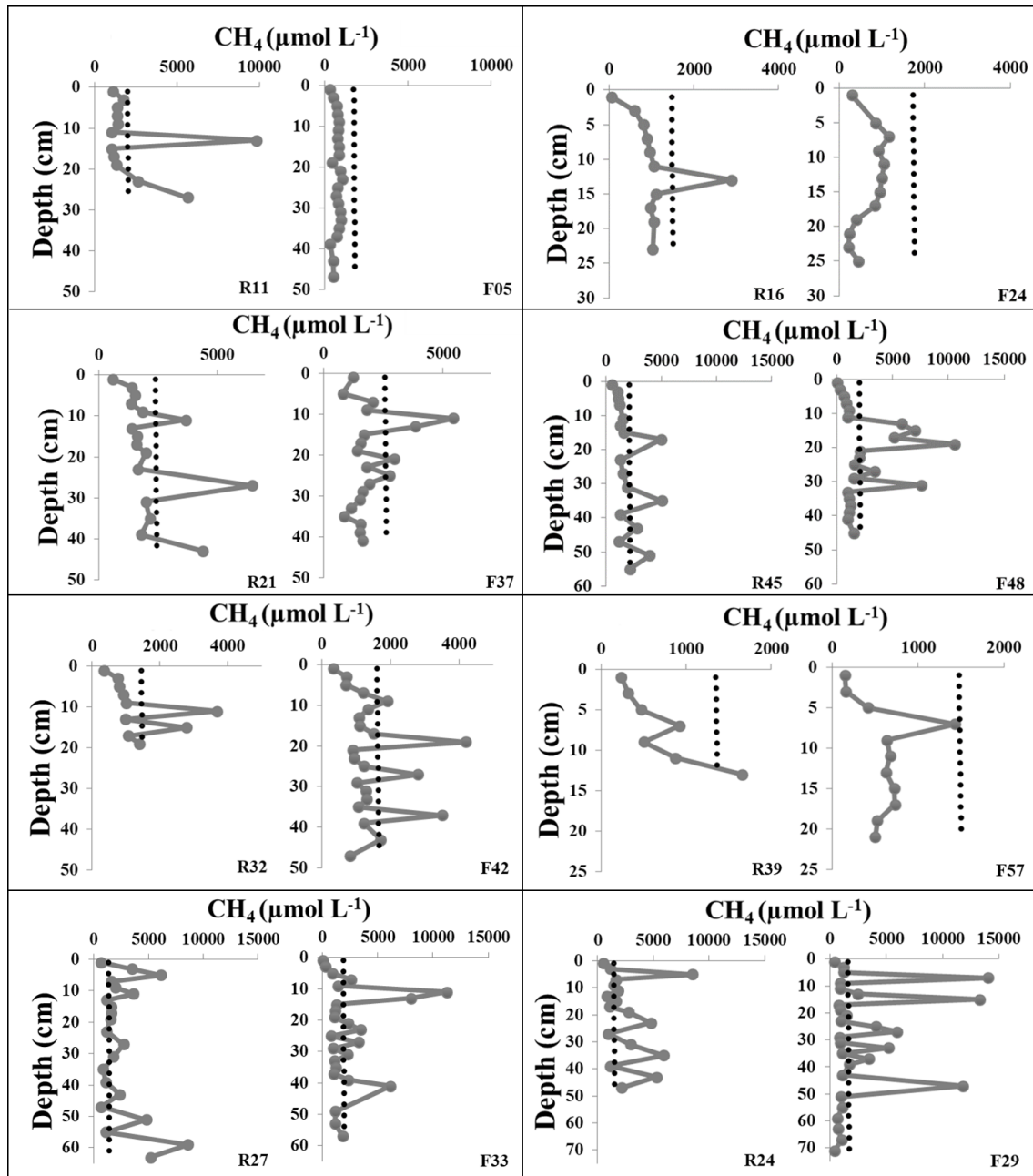
Figure 3. Paired observations of pore water CH₄ profiles during rising (R) and falling

(F) water periods at eight different sampling sites across the reservoir. Black lines

represent the CH₄ saturation concentration (µmol L⁻¹) and grey lines represent the

measured CH₄ concentration (µmol L⁻¹) over sediment depth. The numbers following

the letters F and R correspond to the site codes in **Table S1**.
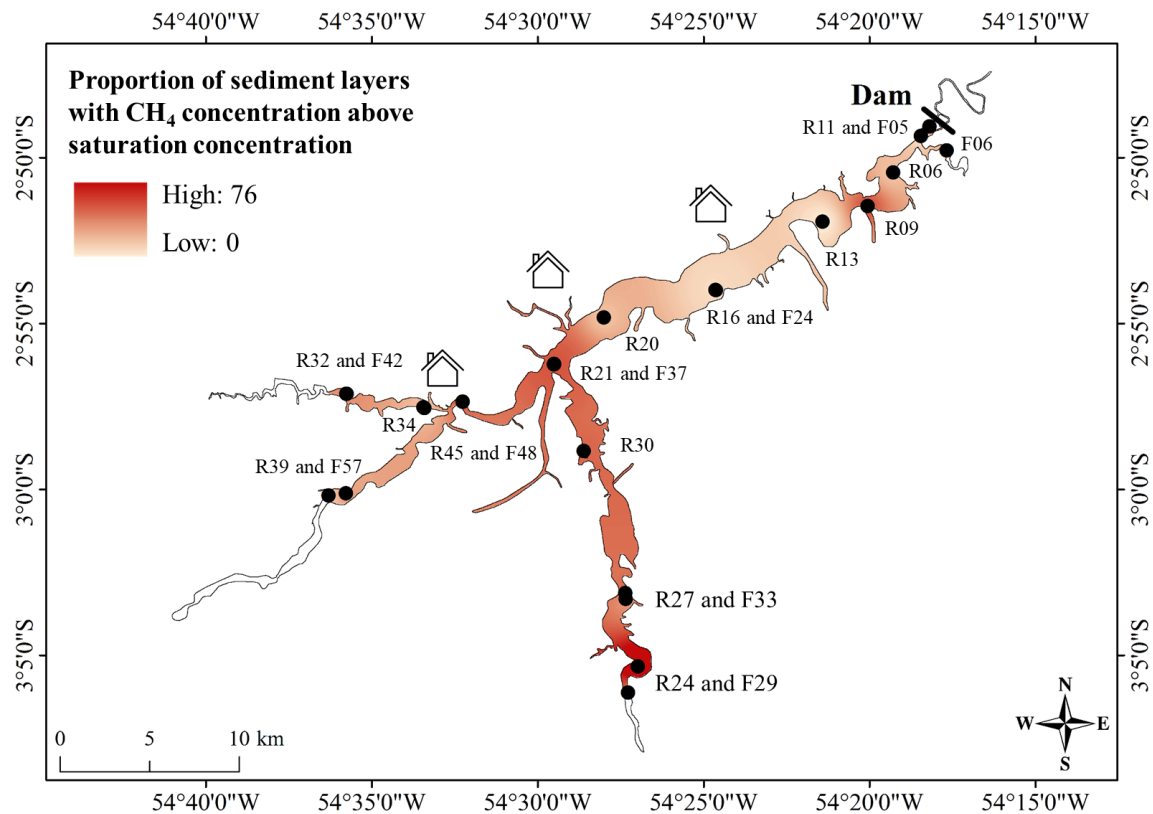
Figure 4. Percentage of sediment layers with CH₄ concentration above saturation. The

black dots represent the sampling sites to produce the interpolation. The houses

represent the settlements at the reservoir.

Discussion

Despite the intense OC mineralization in the tropics, this study found that OC

burial in the sediment of the Amazonian Curuá-Una reservoir was high when compared

to sub-tropical and other tropical reservoirs, probably due to the high carbon inputs

from the forest. However, autochthonous material was also an important component of

CUN sediment. CH_4 concentrations in the sediment pore-water were frequently

supersaturated, indicating that the sediment of CUN also has the potential to emit CH_4

to the atmosphere via ebullition.

328   *SAR and OC burial in an Amazonian reservoir*

329   When a river enters a reservoir, the water flow tends to decrease, favoring the

330   deposition of suspended particles (Fisher, 1983; Scully et al., 2003). Typically, reservoir

331   sedimentation rates are higher in the inflow areas and lower near the shores (Morris and

332   Fan, 1998; Sedláček et al., 2016). CUN showed high SAR near the inflow areas,

333   especially in the main tributary, but in contrast to other reservoirs (e.g. Mendonça et al.,

334   2014), we did not observe any decrease in SAR towards the margins (i.e. the shore). In

335   CUN, sediment accumulation across the entire reservoir area is favored by the shallow

336   topography of the area, and by the presence of dead tree trunks along the reservoir

337   including the margins, which reduce water flow and wave-driven resuspension.

338   Accordingly, our data show that SAR was randomly distributed in relation to the water

339   column depth (**Fig. S5**). Some reservoirs show higher sedimentation rates near the dam,

340   which can be called 'muddy lake area' (Morris and Fan, 1998; Sedláček et al., 2016),

341   and occurs in reservoirs where the fine sediment is transported all the way to the dam

342   (Morris and Fan, 1998; Jenzer Althaus et al., 2009; Sedláček et al., 2016; Schleiss et al.,

343   2016). CUN may be one of those cases (**Fig. 1**), possibly because water retention time is

344   low in the main river channel which is narrow and well separated from the dead tree

345   area, permitting transport of fine-grained sediment until the deeper dam area, where

346   sediments tend to accumulate (Lehman, 1975; Blais and Kalff, 1995). Sediment

347   accumulation was also high at the confluence of the three main tributaries (**Fig. 1**),

348   probably due to sediment deposition as water flow slows down when the rivers enter the

349   main body of the reservoir.

350   Although average SAR in CUN (0.6 cm yr^{-1}) was only slightly higher than that

351   of non-Amazonian reservoirs in Brazil (e.g. Mendonça et al., 2014: 0.5 cm yr^{-1};

352   Franklin et al., 2016: 0.4 cm yr^{-1}), OC burial rates were much higher in CUN than in

353 other hydroelectric reservoirs in the tropics and sub-tropics. For example, OC burial

354 was four times lower in Lake Kariba (23 g C m^{-2} yr^{-1}, Zimbabwe, Kunz et al., 2011) and

355 about two times lower in Mascarenhas de Moraes (42 g C m^{-2} yr^{-1}, Brazil, Mendonça et

356 al., 2014) and other Brazilian reservoirs (40 ± 28 g C m^{-2} yr^{-1}, Brazil, Sikar et al., 2009)

357 when compared to CUN. Even though natural lakes tend to bury OC at lower rates than

358 artificial reservoirs (Mendonça et al., 2017), some Amazonian floodplain lakes showed

359 higher OC burial rates than the CUN reservoir (266 ± 57 g C m^{-2} yr^{-1}; Sanders et al.,

360 2017). This is probably due to their smaller sizes which may result in a higher SAR

361 since there is little area for sediment deposition, but high sediment load from the river

362 during periods of high discharge. While a comparison with the latest global estimate of

363 OC burial in reservoirs – median of 291 g C m^{-2} yr^{-1} (Mendonça et al., 2017) may lead

364 to the conclusion that OC burial in CUN is low, it must be accounted that this global

365 estimate (Mendonça et al., 2017) includes many small agricultural reservoirs (farm

366 ponds), which are generally highly eutrophic systems that receive high sediment inputs

367 from agriculture, resulting in extremely high OC burial rates (Downing et al., 2008).

368 Hence, if compared to other hydroelectric reservoirs at low latitudes, our conclusion

369 remains that OC burial in CUN is high. Importantly, comparisons of average SAR and

370 OC burial rate between studies may be complicated by different sampling schemes, as

371 sedimentation can vary in space and time (Radbourne et al., 2017; Stratton et al., 2019);

372 for example, while in some studies, sites along the margins with zero sedimentation

373 were sampled (e.g. Mendonça et al., 2014; our study), in other studies it was not

374 (Moreira-Turcq et al., 2004; Knoll et al., 2014).

375   The high OC burial in CUN when compared to other low-latitude hydroelectric

376 reservoirs is probably due to the high OC inputs from the productive Amazonian rain

377 forest (Zhang et al., 2017), which compensates the intense sediment mineralization rates

378   caused by high temperature. Using the linear regression model from a compilation of

379   mineralization in freshwater sediments from the literature (Cardoso et al., 2014),

380    $$OC\ mineralization\ = (1.52 + 0.05)\ \times Temperature$$

381   and the average temperature of the bottom water in CUN (29°C), sediment OC

382   mineralization is estimated at a average of 325 g C m^{-2} yr^{-1}. This estimation assumes

383   the same sample size as OC burial (n = 114), and consequently that the random error of

384   each individual prediction (Cardoso et al., 2014) largely averages out and becomes

385   negligible (<1 g C m^{-2} yr^{-1}) for the average of predicted OC mineralization. This

386   estimate of the average sediment OC mineralization rate is in the upper end of the range

387   of values found for Brazilian reservoirs (Cardoso et al., 2014), but may even be

388   conservative given that the CUN reservoir is located in a highly productive biome with

389   high organic matter supply. The total OC deposition rate onto the sediment (OC

390   mineralization + OC burial) of CUN is thus 418 g C m^{-2} yr^{-1}, returning a estimated

391   average OC burial efficiency of 22 % (OC burial efficiency = OC burial / OC deposition

392   rate; Sobek et al., 2009). As expected, due to the positive effect of temperature on

393   mineralization, the estimated average OC burial efficiency in the CUN reservoir is low

394   in comparison to other reservoirs (at least 41% in the tropical lake Kariba (Kunz et al.,

395   2011); average of 67% in the sub-tropical Mascarenhas de Moraes reservoir (Mendonça

396   et al., 2016); average of 87% in the temperate lake Wohlen reservoir (Sobek et al.,

397   2012)). A low OC burial efficiency allows high OC burial only if OC deposition onto

398   the sediment is high enough, and we suggest that the high productivity of the

399   surrounding Amazonian rainforest constitutes a strong OC supply to CUN sediments.

400   The C:N ratio indicates that the sediment OC in CUN consists of a mixture of

401   land-derived and internally-produced OC. The surface sediment C:N ratio varied from

402   10.3 to 17.0 (**Table S3**), and the C:N ratios of phytoplankton are typically 6-9, of

403   aquatic macrophytes >10, of land plants >40 (Meyers and Ishiwatari, 1993; Grasset et

404   al., 2019) and of Amazonian topsoils 10 to 14 (Batjes and Dijkshoorn, 1999). Although

405   we refrained from making quantitative analysis based on C:N ratios, higher C:N values

406   at the river inflow areas (**Fig. 2**) may indicate input from the highly productive

407   watershed and thus the high load of land-derived OC to the sediment. Tropical rain

408   forest is the dominant land cover in the CUN catchment (91%, **Fig. 1**), which may

409   suggest that that the high OC burial rates in CUN are related to a high OC input from

410   the watershed. However, there was no strong relation between OC burial rate and C:N

411   ratio (**Fig. S7A**), even though the C:N ratio has been shown to affect the OC burial

412   efficiency (Sobek et al., 2009). Possibly, the strong effect of SAR on OC burial masked

413   the potential effect of the C:N ratio. In addition, the middle section of the reservoir was

414   characterized by relatively low C:N ratio, indicating a significant share of aquatic OC in

415   the sediment (**Fig. 2**). Likely, the higher water transparency downstream from the river

416   inflow areas due to particle settling stimulate aquatic primary production. Possibly, also

417   sewage input from riverside communities (represented as houses in **Fig. 2**) contributes

418   with N to the reservoir and thus further stimulates aquatic production, since a

419   comparatively low C:N ratio was found near these settlements. Also, even at low C:N

420   ratios, OC burial rates were high (**Fig. S6A**). Hence, it is evident that internally-

421   produced OC makes up an important contribution to the OC buried in the sediments of

422   CUN. The source of buried OC has an important implication in terms of accounting for

423   the sediment carbon as a new sink or not (Prairie et al., 2017), since the burial of aquatic

424   OC can be ascribed to aquatic primary production in the reservoir, which would not

425   have taken place in the absence of the dam, and thus represents a new carbon sink.

426   However, our data do not allow us to make a quantitative estimate of the share of the

427   CUN sediment carbon stock that is of aquatic origin, and thus may be accountable as a

428   new carbon sink resulting from river damming (Prairie et al., 2017).

429   The spatial pattern of OC burial suggests that the catchment size affects

430   sediment load and sedimentation, since the largest sub-catchment (6966 km^2), entering

431   CUN from the south, corresponds with high OC burial rates in the southern river inflow

432   area (**Fig. 1**). The northwestern tributaries, which drain only 2111 and 300 km^2, are not

433   associated with high OC burial in the northeastern tributary (**Fig. 1**), possibly because

434   they are smaller, even though they have a higher share of managed land (34 and 41%,

435   respectively) than the southern sub-catchment (4%). Apparently, even though land

436   management increase erosion (Syvitski and Kettner, 2011), we cannot detect any such

437   effect on sediment OC burial. Also concerning the C:N ratio, an effect of land cover is

438   not evident, since the inflow area of the forest-dominated sub-catchment in the

439   southwest (2855 km^2; 99% forest) had a similar C:N ratio as the tributary of the

440   northwestern sub-catchments, with their higher share of managed land. Possibly, the

441   effect of land cover is masked by other factors affecting sediment OC and C:N, such as

442   internal productivity and local particle settling patterns.

443   Despite being high compared to other hydroelectric reservoirs, OC burial in

444   CUN represents only 15% of the total carbon emission to the atmosphere reported for

445   the CUN reservoir (509 g C m^{-2} yr^{-1}, Duchemin et al., 2000). Similarly, a study

446   conducted in a boreal Canadian reservoir found that OC burial corresponded to 10% of

447   reservoir carbon emission (Teodoru et al., 2012), although burial in other reservoirs can

448   be close to (70%, Mendonça et al., 2014) or even much higher than the total carbon

449   emission to the atmosphere (1600%, Sobek et al., 2012). The magnitudes of carbon

450   burial in relation to the emission in reservoirs depends on many factors (Mendonça et

451   al., 2012). Therefore, although freshwater carbon emission tends to be consistently

452 higher than OC burial in Amazonian freshwater systems (Mendonça et al., 2012), we

453 cannot speculate in how far the results of this study applies to other reservoirs in the

454 Amazon region since many factors affect the carbon processing in inland waters.

455 *High potential for CH_4 ebullition*

456   The high amount of pore water CH_4 profiles with samples above the CH_4

457 saturation concentration indicates a high likelihood of gas bubble formation in most of

458 the sampled sites, and thus the possibility of CH_4 ebullition (**Table S5**). Importantly,

459 however, the link between bubble presence in the sediment and CH_4 ebullition flux is

460 entirely qualitative, and can not be used to estimate the magnitude of CH_4 ebullition.

461 Sites with higher OC burial rate, i.e. river inflow areas, especially the Curuá-Una river,

462 the confluence of the three main rivers and the dam area, also showed a tendency towards

463 higher extent of CH_4 saturation (**Fig. 4**). However, while the relationship between

464 average CH_4 saturation and OC burial at the different sites was positive, it was also

465 weak, but clearly shows the overall high level of CH_4 saturation in CUN sediments

466 (**Fig. 5**). Hence, the CH_4 production in CUN sediments may rather be influenced by the

467 OC supply rate to anaerobic sediment layers than by the reactivity of the sediment OC,

468 since there was no association between the C:N ratio and the extent of CH_4 saturation

469 (**Fig. S7B**). Links between high sedimentation rate and sediment CH_4 pore water

470 concentration as well as CH_4 ebullition have been reported previously (Sobek et al.,

471 2012; Maeck et al., 2013), and in addition, fresh land plant-derived organic matter such

472 as leaves transported by the rivers may fuel substantial CH_4 production at anoxic

473 conditions (Grasset et al., 2018). This highlights that sediment accumulation bottoms

474 close to river inflow areas can be prone to exhibit high CH_4 ebullition (DelSontro et al.,

475 2011), not least because the shallow water column in inflow areas (**Fig. S6**) facilitates

476 CH_4 bubble transport to the atmosphere.
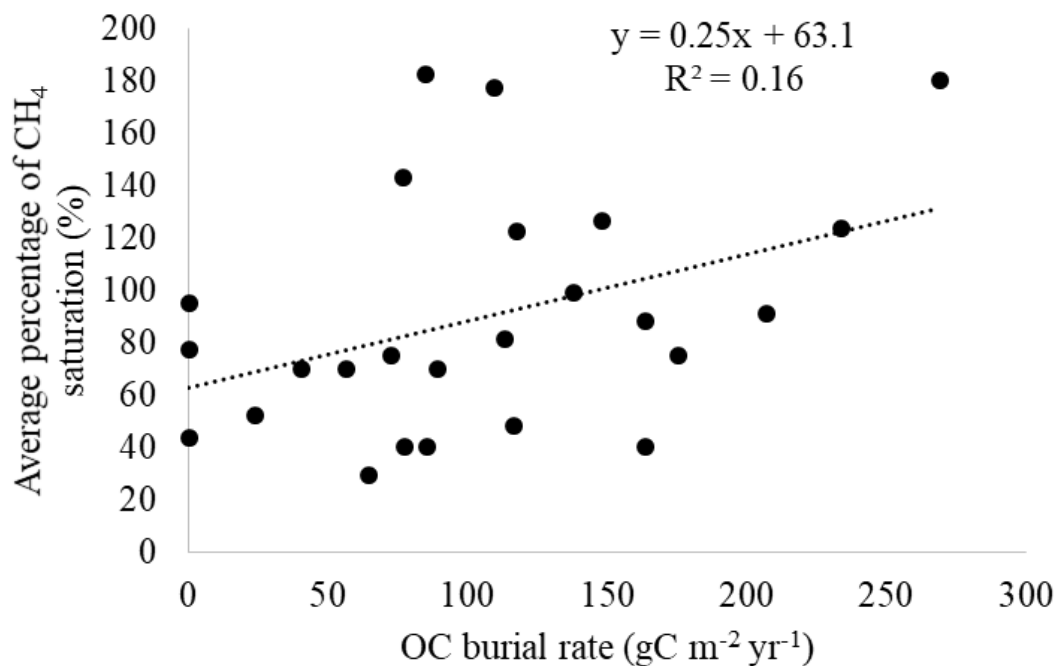
Figure 5. Regression model of average percentage of CH_4 saturation (%) in the sediment pore water and OC burial rate (g C m^{-2} yr^{-1}). Each circle represents one sampling site.

Compared to other reservoirs, CUN had a higher share of sites (20 of 25) with pore water CH_4 concentration over the saturation threshold. In the Mascarenhas de Morais reservoir (Brazil), 6 of 16 sites with pore water CH_4 concentration over the saturation threshold were found (Mendonça et al., 2016). In Lake Wohlen (Switzerland), 4 of 8 sites with pore water CH_4 concentration over the threshold were found (Sobek et al., 2012). However, these differences should be interpreted with caution. Using the 100% saturation concentration as a threshold may underestimate the potential for ebullition, since changes in the pressure may result in bubbles release during sediment sampling, especially in layers above 100% saturation. Therefore, our results of the degree of pore water CH_4 saturation, as well as the results from the literature cited above, are conservative.

492   We did not find statistical difference between CH_4 pore water concentration

493   during rising and falling periods (**Fig. 3**), although other studies suggest a strong

494   influence of water level or pressure changes on CH_4 ebullition (Mattson and Likens,

495   1990; Eugster et al., 2011; Maeck et al., 2014). Interestingly, 2 of the 8 sites with

496   generally low CH_4 pore water concentration were low at both sampling occasions,

497   indicating that there may be an important spatial component in sediment CH_4

498   production and saturation (**Fig. 3**, sites F24 x R16 and F57 x R39), which however was

499   not related to the C:N ratio or OC burial rate at these sites.

500   **Conclusions**

501   The comparatively high OC burial rate of the Amazonian CUN reservoir

502   probably results from high OC deposition onto the sediment, since the warm water (28-

503   30°C) implies a high sediment OC mineralization rate. The forest seems to be a major

504   OC source to the reservoir although the relatively low C:N ratio in some parts of the

505   reservoir suggests an also significant aquatic contribution to sediment OC burial. In

506   some parts of the reservoir, particularly in the river inflow areas, sediments are probably

507   a CH_4 source by ebullition. Therefore, large inputs from a highly productive forest

508   probably boost the OC burial rate, as well as CH_4 production, with a still unknown net

509   effect on the regional carbon budget. Given the planned expansion of hydropower dams

510   in the Amazon region, and the high OC burial rate in CUN shown here, future studies

511   should quantify how OC burial and CH_4 emission may be affected by new Amazonian

512   hydroelectric reservoirs. Moreover, it will be critical to quantify the effect of the new

513   Amazonian reservoirs on the ocean's carbon budget, since the CUN dam alone retains

514   yearly 7,500 tons of OC and a part of it would likely reach the ocean in the absence of

515   the dam.

516   **Data availability.** All the data used in this study can be found in the manuscript and in

517   the Supplement.

518   **Author contributions.** GRQ, JRP, AI, RM, RV carried out the sampling campaings.

519   GRQ processed the data. AI analyzed the samples. GRQ and JRP prepared the figures.

520   RM, SS, FR designed the study. All authors contributed to interpreting data and writing

521   the manuscript.

522   **Competing interests.** The authors declare that they have no conflict of interest.

523   **Acknowledgments.** The research leading to these results has received funding from the

524   European Research Council under the European Union's Seventh Framework

525   Programme (FP7/2007–2013)/ERC grant agreement n° 336642. S.S. received additional

526   support by the program *Pesquisador Visitante Especial*, *Ciência sem Fronteiras*, n°

527   401384/2014-4. This study was also financed in part by the *Coordenação de*

528   *Aperfeiçoamento de Pessoal de Nível Superior* (CAPES) - Finance Code 001. F.R. has

529   been supported by the *Conselho Nacional de Desenvolvimento Científico e Tecnológico*

530   (CNPq; grant no. 401384/2014-4). We are thankful for the support from

531   ELETRONORTE during the field campaigns.

532   **References**

533   Aben, R. C., Barros, N., Van Donk, E., Frenken, T., Hilt, S., Kazanjian, G., Lamers, L.

534   P., Peeters, E. T., Roelofs, J. G., and de Senerpont Domis, L. N.: Cross continental

535   increase in methane ebullition under climate change, Nature communications, 8, 1682,

536   2017.

537   Almeida, R. M., Barros, N., Cole, J. J., Tranvik, L., and Roland, F.: Emissions from

538   Amazonian dams, Nature Climate Change, 3, 1005, 2013.

539   Almeida, R. M., Shi, Q., Gomes-Selman, J. M., Wu, X., Xue, Y., Angarita, H., Barros,

540   N., Forsberg, B. R., García-Villacorta, R., Hamilton, S. K., Melack, J. M., Montoya, M.,

541   Perez, G., Sethi, S. A., Gomes, C. P., Flecker, A. S. Reducing greenhouse gas emissions

542   of Amazon hydropower with strategic dam planning. Nature communications, 10, 1-9.

543   2019.

544   Barros, N., Cole, J. J., Tranvik, L. J., Prairie, Y. T., Bastviken, D., Huszar, V. L., Del

545   Giorgio, P., and Roland, F.: Carbon emission from hydroelectric reservoirs linked to

546   reservoir age and latitude, Nature Geoscience, 4, 593, 2011.

547   Batjes, N. H., and Dijkshoorn, J. A.: Carbon and nitrogen stocks in the soils of the

548   Amazon Region, Geoderma, 89, 273-286, 1999.

549   Blais, J. M., and Kalff, J.: The influence of lake morphometry on sediment focusing,

550   Limnology and Oceanography, 40, 582-588, 1995.

551   Cardoso, S. J., Enrich-Prast, A., Pace, M. L., and Roland, F.: Do models of organic

552   carbon mineralization extrapolate to warmer tropical sediments?, Limnology and

553   Oceanography, 59, 48-54, 2014.

554   Cole, J. J., Prairie, Y. T., Caraco, N. F., McDowell, W. H., Tranvik, L. J., Striegl, R. G.,

555   Duarte, C. M., Kortelainen, P., Downing, J. A., and Middelburg, J. J.: Plumbing the

556   global carbon cycle: integrating inland waters into the terrestrial carbon budget,

557   Ecosystems, 10, 172-185, 2007.

558   da Silva Soito, J. L., and Freitas, M. A. V.: Amazon and the expansion of hydropower

559   in Brazil: Vulnerability, impacts and possibilities for adaptation to global climate

560   change, Renewable and Sustainable Energy Reviews, 15, 3165-3177, 2011.

561 Deemer, B. R., Harrison, J. A., Li, S., Beaulieu, J. J., DelSontro, T., Barros, N.,

562 Bezerra-Neto, J. F., Powers, S. M., Dos Santos, M. A., and Vonk, J. A.: Greenhouse gas

563 emissions from reservoir water surfaces: a new global synthesis, BioScience, 66, 949-

564 964, 2016.

565 DelSontro, T., Boutet, L., St-Pierre, A., del Giorgio, P. A., and Prairie, Y. T.: Methane

566 ebullition and diffusion from northern ponds and lakes regulated by the interaction

567 between temperature and system productivity, Limnology and Oceanography, 61, S62-

568 S77, 2016.

569 DelSontro, T., Kunz, M. J., Kempter, T., Wüest, A., Wehrli, B., and Senn, D. B.: Spatial

570 heterogeneity of methane ebullition in a large tropical reservoir, Environmental science

571 & technology, 45, 9866-9873, 2011.

572 Downing, J. A., Cole, J. J., Duarte, C., Middelburg, J. J., Melack, J. M., Prairie, Y. T.,

573 Kortelainen, P., Striegl, R. G., McDowell, W. H., and Tranvik, L. J.: Global abundance

574 and size distribution of streams and rivers, Inland waters, 2, 229-236, 2012.

575 Downing, J. A., Cole, J. J., Middelburg, J. J., Striegl, R. G., Duarte, C. M., Kortelainen,

576 P., Prairie, Y. T., and Laube, K. A.: Sediment organic carbon burial in agriculturally

577 eutrophic impoundments over the last century, Global Biogeochemical Cycles, 22,

578 2008.

579 Duchemin, É., Lucotte, M., Canuel, R., Queiroz, A. G., Almeida, D. C., Pereira, H. C.,

580 and Dezincourt, J.: Comparison of greenhouse gas emissions from an old tropical

581 reservoir with those from other reservoirs worldwide. Internationale Vereinigung für

582 theoretische und angewandte Limnologie: Verhandlungen, 27, 1391-1395, 2000.

583   Eugster, W., DelSontro, T., and Sobek, S.: Eddy covariance flux measurements confirm

584   extreme CH_4 emissions from a Swiss hydropower reservoir and resolve their short-term

585   variability. Biogeosciences, 8, 2815-2831, 2011.

586   Fearnside, P. M., and Pueyo, S.: Greenhouse-gas emissions from tropical dams, Nature

587   Climate Change, 2, 382, 2012.

588   Fearnside, P. M.: Do hydroelectric dams mitigate global warming? The case of Brazil's

589   Curuá-Una Dam, Mitigation and Adaptation Strategies for Global Change, 10, 675-691,

590   2005.

591   Fisher, R. V.: Flow transformations in sediment gravity flows, Geology, 11, 273-274,

592   1983.

593   Franklin, R. L., Fávaro, D. I. T., and Damatto, S. R.: Trace metal and rare earth

594   elements in a sediment profile from the Rio Grande Reservoir, Sao Paulo, Brazil:

595   determination of anthropogenic contamination, dating, and sedimentation rates, Journal

596   of Radioanalytical and Nuclear Chemistry, 307, 99-110, 2016.

597   Gälman, V., Rydberg, J., de-Luna, S. S., Bindler, R., and Renberg, I.: Carbon and

598   nitrogen loss rates during aging of lake sediment: changes over 27 years studied in

599   varved lake sediment, Limnology and Oceanography, 53, 1076-1082, 2008.

600   Grasset, C., Abril, G., Mendonça, R., Roland, F., and Sobek, S.: The transformation of

601   macrophyte-derived organic matter to methane relates to plant water and nutrient

602   contents, Limnology and Oceanography, 2019.

603   Grasset, C., Mendonça, R., Villamor Saucedo, G., Bastviken, D., Roland, F., and Sobek,

604   S.: Large but variable methane production in anoxic freshwater sediment upon addition

605   of allochthonous and autochthonous organic matter, Limnology and oceanography, 63,

606   1488-1501, 2018.

607   HydroBASINS: https://www.hydrosheds.org/page/hydrobasins, 2019.

608   IPCC: Stocker, T. F., Qin, D., Plattner, G. K., Tignor, M., Allen, S. K., Boschung, J.,

609   Nauels, A., Xia, Y., Bex, V., Midgley, P. M. Climate change 2013: The physical science

610   basis, 2013.

611   Jenzer Althaus, J., De Cesare, G., Boillat, J.-L., and Schleiss, A.: Turbidity currents at

612   the origin of reservoir sedimentation, case studies, Proceedings (on CD) of the 23rd

613   Congress of the Int. Commission on Large Dams CIGB-ICOLD, 58-60, 2009.

614   Knoll, L. B., Vanni, M. J., Renwick, W. H., and Kollie, S.: Burial rates and

615   stoichiometry of sedimentary carbon, nitrogen and phosphorus in M idwestern US

616   reservoirs, Freshwater biology, 59, 2342-2353, 2014.

617   Kortelainen, P., Rantakari, M., Pajunen, H., Huttunen, J. T., Mattsson, T., Juutinen, S.,

618   Larmola, T., Alm, J., Silvola, J., and Martikainen, P. J.: Carbon evasion/accumulation

619   ratio in boreal lakes is linked to nitrogen, Global Biogeochemical Cycles, 27, 363-374,

620   2013.

621   Kunz, M. J., Anselmetti, F. S., Wüest, A., Wehrli, B., Vollenweider, A., Thüring, S.,

622   and Senn, D. B.: Sediment accumulation and carbon, nitrogen, and phosphorus

623   deposition in the large tropical reservoir Lake Kariba (Zambia/Zimbabwe), Journal of

624   Geophysical Research: Biogeosciences, 116, 2011.

625   Lehman, J. T.: Reconstructing the Rate of Accumulation of Lake Sediment: The Effect

626   of Sediment Focusing 1, Quaternary Research, 5, 541-550, 1975.

627   Liu, L., Wilkinson, J., Koca, K., Buchmann, C., and Lorke, A.: The role of sediment

628   structure in gas bubble storage and release, Journal of Geophysical Research:

629   Biogeosciences, 121, 1992-2005, 2016.

630   Maeck, A., DelSontro, T., McGinnis, D. F., Fischer, H., Flury, S., Schmidt, M., Fietzek,

631   P., and Lorke, A.: Sediment trapping by dams creates methane emission hot spots,

632   Environmental science & technology, 47, 8130-8137, 2013.

633   Maeck, A., Hofmann, H., and Lorke, A.: Pumping methane out of aquatic sediments:

634   Ebullition forcing mechanisms in an impounded river, Biogeosciences, 11, 2925-2938,

635   2014.

636   Marotta, H., Pinho, L., Gudasz, C., Bastviken, D., Tranvik, L. J., and Enrich-Prast, A.:

637   Greenhouse gas production in low-latitude lake sediments responds strongly to

638   warming, Nature Climate Change, 4, 467, 2014.

639   Mattson, M. D., and Likens, G. E.: Air pressure and methane fluxes. Nature, 347, 718,

640   1990.

641   McGinnis, D. F., Greinert, J., Artemov, Y., Beaubien, S., and Wüest, A.: Fate of rising

642   methane bubbles in stratified waters: How much methane reaches the atmosphere?,

643   Journal of Geophysical Research: Oceans, 111, 2006.

644   Mendonça, R., Kosten, S., Sobek, S., Barros, N., Cole, J. J., Tranvik, L., and Roland, F.:

645   Hydroelectric carbon sequestration, Nature Geoscience, 5, 838, 2012.

646   Mendonça, R., Kosten, S., Sobek, S., Cardoso, S. J., Figueiredo-Barros, M. P., Estrada,

647   C. H. D., and Roland, F.: Organic carbon burial efficiency in a large tropical

648   hydroelectric reservoir, Biogeosciences, 13, 3331-3342, 2016.

649   Mendonça, R., Kosten, S., Sobek, S., Cole, J. J., Bastos, A. C., Albuquerque, A. L.,

650   Cardoso, S. J., and Roland, F.: Carbon sequestration in a large hydroelectric reservoir:

651   an integrative seismic approach, Ecosystems, 17, 430-441, 2014.

652   Mendonça, R., Müller, R. A., Clow, D., Verpoorter, C., Raymond, P., Tranvik, L. J.,

653   and Sobek, S.: Organic carbon burial in global lakes and reservoirs, Nature

654   communications, 8, 1694, 2017.

655   Meyers, P. A., and Ishiwatari, R.: Lacustrine organic geochemistry—an overview of

656   indicators of organic matter sources and diagenesis in lake sediments, Organic

657   geochemistry, 20, 867-900, 1993.

658   Middelburg, J. J., Vlug, T., Jaco, F., and Van der Nat, W. A.: Organic matter

659   mineralization in marine systems, Global and Planetary Change, 8, 47-58, 1993.

660   Moreira-Turcq, P., Jouanneau, J., Turcq, B., Seyler, P., Weber, O., and Guyot, J.-L.:

661   Carbon sedimentation at Lago Grande de Curuai, a floodplain lake in the low Amazon

662   region: insights into sedimentation rates, Palaeogeography, Palaeoclimatology,

663   Palaeoecology, 214, 27-40, 2004.

664   Morris, G. L., and Fan, J.: Reservoir sedimentation handbook: design and management

665   of dams, reservoirs, and watersheds for sustainable use, McGraw Hill Professional,

666   1998.

667   Mulholland, P. J., and Elwood, J. W.: The role of lake and reservoir sediments as sinks

668   in the perturbed global carbon cycle, Tellus, 34, 490-499, 1982.

669   Paranaíba, J. R., Barros, N., Mendonça, R., Linkhorst, A., Isidorova, A., Roland, F.,

670   Almeida, R. M., and Sobek, S.: Spatially resolved measurements of CO_2 and CH_4

671 concentration and gas-exchange velocity highly influence carbon-emission estimates of

672 reservoirs, Environmental science & technology, 52, 607-615, 2018.

673 Prairie, Y. T., Alm, J., Beaulieu, J., Barros, N., Battin, T., Cole, J., Del Giorgio, P.,

674 DelSontro, T., Guérin, F., and Harby, A.: Greenhouse gas emissions from freshwater

675 reservoirs: what does the atmosphere see?, Ecosystems, 1-14, 2017.

676 Quadra, G. R., Lino, A., Sobek, A., Malm, O., Barros, N., Guida, Y., Thomaz, J.,

677 Mendonça, R., Cardoso, S., Estrada, C., Rust, F., and Roland, F.: Environmental Risk of

678 Metal Contamination in Sediments of Tropical Reservoirs. Bulletin of Environmental

679 Contamination and Toxicology, 1-10, 2019.

680 Radbourne, A. D., Ryves, D. B., Anderson, N. J., and Scott, D. R.: The historical

681 dependency of organic carbon burial efficiency, Limnology and Oceanography, 62,

682 1480-1497, 2017.

683 Raymond, P. A., Hartmann, J., Lauerwald, R., Sobek, S., McDonald, C., Hoover, M.,

684 Butman, D., Striegl, R., Mayorga, E., and Humborg, C.: Global carbon dioxide

685 emissions from inland waters, Nature, 503, 355, 2013.

686 Renwick, W. H., Smith, S. V., Bartley, J. D., and Buddemeier, R. W.: The role of

687 impoundments in the sediment budget of the conterminous United States.

688 Geomorphology, 71, 99-111, 2005.

689 Sanders, L. M., Taffs, K. H., Stokes, D. J., Sanders, C. J., Smoak, J. M., Enrich-Prast,

690 A., Macklin, P. A., Santos, I. R., and Marotta, H.: Carbon accumulation in Amazonian

691 floodplain lakes: A significant component of Amazon budgets?, Limnology and

692 Oceanography Letters, 2, 29-35, 2017.

693   Schleiss, A. J., Franca, M. J., Juez, C., and De Cesare, G.: Reservoir sedimentation,

694   Journal of Hydraulic Research, 54, 595-614, 2016.

695   Scully, M., Friedrichs, C. T., and Wright, L.: Numerical modeling of gravity-driven

696   sediment transport and deposition on an energetic continental shelf: Eel River, northern

697   California, Journal of Geophysical Research: Oceans, 108, 2003.

698   Sedláček, J., Bábek, O., and Kielar, O.: Sediment accumulation rates and high-

699   resolution stratigraphy of recent fluvial suspension deposits in various fluvial settings,

700   Morava River catchment area, Czech Republic, Geomorphology, 254, 73-87, 2016.

701   Segers, R.: Methane production and methane consumption: a review of processes

702   underlying wetland methane fluxes. Biogeochemistry, 41, 23-51, 1998.

703   Sikar, E., Matvienko, B., Santos, M., Rosa, L., Silva, M., Santos, E., Rocha, C., and

704   Bentes Jr, A.: Tropical reservoirs are bigger carbon sinks than soils, Internationale

705   Vereinigung für theoretische und angewandte Limnologie: Verhandlungen, 30, 838-

706   840, 2009.

707   Sobek, S., DelSontro, T., Wongfun, N., and Wehrli, B.: Extreme organic carbon burial

708   fuels intense methane bubbling in a temperate reservoir, Geophysical Research Letters,

709   39, 2012.

710   Sobek, S., Durisch-Kaiser, E., Zurbrügg, R., Wongfun, N., Wessels, M., Pasche, N., and

711   Wehrli, B.: Organic carbon burial efficiency in lake sediments controlled by oxygen

712   exposure time and sediment source, Limnology and Oceanography, 54, 2243-2254,

713   2009.

714   Sobek, S., Zurbrügg, R., and Ostrovsky, I.: The burial efficiency of organic carbon in

715   the sediments of Lake Kinneret, Aquatic sciences, 73, 355-364, 2011.

716   Stratton, L. E., Haggerty, R., and Grant, G. E.: The Importance of Coarse Organic

717   Matter and Depositional Environment to Carbon Burial Behind Dams in Mountainous

718   Environments. Journal of Geophysical Research: Earth Surface, 124, 2118-2140, 2019.

719   Syvitski, J. P., and Kettner, A.: Sediment flux and the Anthropocene. Philosophical

720   Transactions of the Royal Society A: Mathematical, Physical and Engineering Sciences,

721   369, 957-975, 2011.

722   Team, R. C. R: A language and environment for statistical computing. Vienna, Austria:

723   R Foundation for Statistical Computing; 2017, ISBN3-900051-07-0 https://www. R-

724   project. Org.

725   Teodoru, C. R., Bastien, J., Bonneville, M. C., del Giorgio, P. A., Demarty, M.,

726   Garneau, M., Hélie, J. F., Pelletier, L., Prairie, Y. T., and Roulet, N. T.: The net carbon

727   footprint of a newly created boreal hydroelectric reservoir, Global Biogeochemical

728   Cycles, 26, 2012.

729   Tranvik, L. J., Downing, J. A., Cotner, J. B., Loiselle, S. A., Striegl, R. G., Ballatore, T.

730   J., Dillon, P., Finlay, K., Fortino, K., and Knoll, L. B.: Lakes and reservoirs as

731   regulators of carbon cycling and climate, Limnology and Oceanography, 54, 2298-

732   2314, 2009.

733   Verpoorter, C., Kutser, T., Seekell, D. A., and Tranvik, L. J.: A global inventory of

734   lakes based on high-resolution satellite imagery, Geophysical Research Letters, 41,

735   6396-6402, 2014.

736   Vörösmarty, C. J., Meybeck, M., Fekete, B., Sharma, K., Green, P., and Syvitski, J. P.:

737   Anthropogenic sediment retention: major global impact from registered river

738   impoundments, Global and planetary change, 39, 169-190, 2003.

739   Wik, M., Thornton, B. F., Bastviken, D., MacIntyre, S., Varner, R. K., and Crill, P. M.:

740   Energy input is primary controller of methane bubbling in subarctic lakes, Geophysical

741   Research Letters, 41, 555-560, 2014.

742   Winemiller, K. O., McIntyre, P. B., Castello, L., Fluet-Chouinard, E., Giarrizzo, T.,

743   Nam, S., Baird, I., Darwall, W., Lujan, N., and Harrison, I.: Balancing hydropower and

744   biodiversity in the Amazon, Congo, and Mekong, Science, 351, 128-129, 2016.

745   Yvon-Durocher, G., Allen, A. P., Bastviken, D., Conrad, R., Gudasz, C., St-Pierre, A.,

746   Thanh-Duc, N., and Del Giorgio, P. A.: Methane fluxes show consistent temperature

747   dependence across microbial to ecosystem scales, Nature, 507, 488, 2014.

748   Zarfl, C., Lumsdon, A. E., Berlekamp, J., Tydecks, L., and Tockner, K.: A global boom

749   in hydropower dam construction, Aquatic Sciences, 77, 161-170, 2015.

750   Zhang, Y., Xiao, X., Wu, X., Zhou, S., Zhang, G., Qin, Y., and Dong, J.: A global

751   moderate resolution dataset of gross primary production of vegetation for 2000–2016,

752   Scientific data, 4, 2017.